

Research Article

# Biogenically Synthesized ZnO and Cu-Doped ZnO Nanoparticles: Effect of Cu-Dopant Concentration and Annealing on Morphology and Optical Properties

Parameswaran Parlikad Subramanian\* , Rethikala Pandikkappallil Kumaran ,  
Manoj Nageri 

Postgraduate Department of Chemistry and Research Center, Sanatana Dharma College, University of Kerala, Alappuzha, India

## Abstract

In this work, ZnO nanoparticles and Cu-doped ZnO nanoparticles were biogenically synthesized using precipitation method in *Cissus quadrangularis* plant extract medium. The influence of Cu dopant on the crystalline structure, optical properties, and morphology of ZnO was investigated. The samples were characterized by XRD, FTIR, UV-vis spectroscopy and SEM. XRD patterns confirmed the wurtzite formation of doped and undoped ZnO nanoparticles. The average crystallite size of the neat and Cu-doped samples was ~18 nm irrespective of the amount of dopant. The annealing process enhanced the size of both the neat and Cu-doped samples. However, the influence on the size is less prominent in the Cu-doped sample than in the neat sample. The UV-visible spectral analysis shows that all the synthesized doped and undoped nano zinc oxides absorb at ~400nm. The band gap energy of Cu-doped ZnO particles was greater for unannealed samples whereas it was appreciably lowered on annealing for Cu-doped samples. SEM analysis shows rod-like morphology for the unannealed and annealed undoped zinc oxides. It is changed to flower-like morphology with the addition of 5mM Cu<sup>2+</sup> and then to nano sheet-like structure with the incorporation of higher amount of Cu<sup>2+</sup> ions. Annealing of zinc oxide samples leads to the smoothening of the surfaces with a change in morphology for the ZnO nanoparticles.

## Keywords

Green Synthesis, Nano Zinc Oxide, *Cissus quadrangularis*

## 1. Introduction

Zinc oxide (ZnO) is a typical electronic and photonic wurtzite n-type semiconductor with a wide direct band gap of 3.37eV and a high exciton binding energy (60 meV) at room temperature [1]. Its excellent properties as a semiconductor material like high electron mobility, high thermal conductivity, good transparency, wide direct band gap (3.37eV), large ex-

citon binding energy and easiness of growing in the nanostructure form, make ZnO suitable for applications such as nanogenerators, gas sensors, biosensors, solar cells, varistors, photodetectors and photocatalysts [2-4].

ZnO is an interesting semiconductor material having a Hexagonal Close Packing (hcp) lattice with empty octahedral

\*Corresponding author: [psp@sdcollege.in](mailto:psp@sdcollege.in) (Parameswaran Parlikad Subramanian)

Received: 23 June 2024; Accepted: 11 July 2024; Published: 29 July 2024



Copyright: © The Author(s), 2024. Published by Science Publishing Group. This is an **Open Access** article, distributed under the terms of the Creative Commons Attribution 4.0 License (<http://creativecommons.org/licenses/by/4.0/>), which permits unrestricted use, distribution and reproduction in any medium, provided the original work is properly cited.

sites. Plenty of sites available in ZnO can be accommodated by intrinsic defects and extrinsic dopants [5]. Doping of selective elements in ZnO nanoparticles is an effective way to modify or tune the optical, electrical, magnetic and catalytic properties of ZnO. The optical properties of ZnO nanoparticles can be tuned by incorporating various ions such as alkaline earth metal ions, transition metal ions and rare earth metal ions into the crystal lattice [6, 7]. Copper is used as the dopant, since high conductivity, cheap and availability on Earth's crust. Copper has a similar electronic shell structure with zinc and possesses high solubility in ZnO. Cu could produce p-type ZnO by introducing an acceptor energy level in ZnO with energy 0.45 eV above the valence band [8]. The doping of Cu in ZnO is expected to modify absorption, and other physical or chemical properties of ZnO [8, 9]. Doping of ZnO with copper was intended to enhance the surface defects of ZnO. These can subsequently be used as efficient centres for optical absorption.

Various approaches for the preparation of ZnO nanoparticles (ZnONP) have been developed, namely, sol-gel, microemulsion, thermal decomposition of organic precursor, spray pyrolysis, electrodeposition, ultrasonic, microwave-assisted techniques, chemical vapour deposition and hydrothermal and precipitation methods [10, 11]. However, biological methods for the synthesis of ZnONP using microorganisms, enzymes, and plant extracts have been suggested as possible eco-friendly alternatives to chemical and physical methods [12-15].

Across the tropical world, *Cissus quadrangularis* is a perennial herb with therapeutic qualities. In India, it is one of the most widely utilized medicinal plants. The plant is said to be indigenous to West Africa, Java, Malaysia, Sri Lanka, and India. *Cissus quadrangularis* can be used for treating diabetes, obesity, high cholesterol, bone fractures, allergies, cancer, stomach upset, painful menstrual periods, asthma, malaria, wound healing, peptic ulcer disease, osteoporosis and as an anabolic steroid [16].

This work aims at the synthesis of ZnONP and Copper doped (Cu-doped) ZnONP samples with varying amounts of dopant, via the precipitation method using *Cissus quadrangularis* plant extract and compare the optical and the morphological features of the synthesized ZnONP samples.

## 2. Materials and Methods

Zinc nitrate hexahydrate, Copper sulphate pentahydrate and Sodium Hydroxide were used in the experiments. All the AR grade chemicals used were obtained from E. Merck (Mumbai, India) and were applied without more purification. Deionized water is used for the preparation of solutions and *Cissus quadrangularis* plants were collected from Sanatana Dharma College Campus, Alappuzha, Kerala.

### 2.1. Preparation of *Cissus quadrangularis* Plant Extract

Fresh *Cissus quadrangularis* plants were collected. Washed thoroughly with water to remove the impurities. About 5g of sliced stem was taken in a 250 mL glass beaker with 100 mL distilled water. The mixture was then heated at 60 °C for a few minutes until the aqueous solution changed from watery to light greenish yellow. The extract was then cooled to room temperature and filtered using Whatmann no: 1 filter paper.

### 2.2. Synthesis of ZnO Nanoparticles

Synthesis of ZnONPs in green medium (ZnONPG): 250 ml 0.05M Zinc Nitrate hexahydrate solution was taken in a 500ml beaker. 2ml aqueous extract of the *Cissus quadrangularis* plant was introduced into it. 1.0M NaOH solution was added at room temperature drop by drop to reach pH 12 (~20ml NaOH solution), with constant stirring. After the addition, it was stirred for about 2 hours. After completion of the reaction, the white precipitate formed was washed thoroughly with distilled water followed by ethanol to remove impurities. The precipitate was then dried in a hot air oven for 6 hours at 100 °C.

Synthesis of Cu-doped ZnONPs in green medium (ZnONPGCu): Various concentrations of zinc nitrate and copper sulphate i.e. 0.0450M  $Zn(NO_3)_2$  & 0.0050M (5mM)  $CuSO_4$ ; 0.0425M  $Zn(NO_3)_2$  & 0.0075M (7.5mM)  $CuSO_4$  and finally 0.04M  $Zn(NO_3)_2$  & 0.01M (10mM)  $CuSO_4$  in 250ml water were taken for the synthesis of Cu-doped ZnO samples. The method used above was adopted to synthesis Cu-doped ZnONPs. Each sample was designated as ZnONPGCu(5), ZnONPGCu(7.5) and ZnONPGCu(10) respectively.

The synthesized samples were annealed at 350 °C and 700 °C for 2 hours. These samples were designated as ZnONPG350, ZnONPG700, ZnONPGCu(5)350, ZnONPGCu(5)700, ZnONPGCu(7.5)350, ZnONPGCu(7.5)700, ZnONPGCu(10)350 and ZnONPGCu(10)700.

### 2.3. Characterization Methods

Scanning electron microscopy: VEGA3 TESCAN analyzer with acceleration voltage 10 KV was used to take the images of biosynthesized zinc oxide nanoparticles.

X-Ray Diffractogram: Analysis of the synthesized zinc oxide nanoparticles is carried out using X-Ray Diffractometer - Bruker AXS D8 Advance, with Cu k-alpha radiation of wavelength 1.5402 Å.

UV-vis spectral analysis: UV-visible analysis of the samples was done using a UV 2600 Shimadzu instrument.

FTIR: FTIR spectra of ZnONP samples were taken in Thermo Nicolet Avatar 370 FTIR spectrophotometer (spectral range 4000-400  $cm^{-1}$  with KBr beam splitter)

### 3. Results and Discussion

#### 3.1. Solubility

Figure 1 shows the solubility of ZnONPG and Cu-doped sample in Dimethylsulphoxide (DMSO). The image shows that ZnONPG is soluble in DMSO while the Cu-doped sample is partially soluble. The presence of copper in zinc oxide makes it partially insoluble.



Figure 1. Solubility of ZnONPG and ZnONPGCu(5) in DMSO.

#### 3.2. FT-IR Spectroscopy

Figure 2. represents the FTIR spectra of ZnONPG and ZnONPGCu(7.5). Both the samples show peaks at  $\sim 434 \text{ cm}^{-1}$ .

This is due to the Zn-O stretching. The absorption peak at  $\sim 1380 \text{ cm}^{-1}$  corresponds to H-O-H vibrations and the band observed at  $\sim 860 \text{ cm}^{-1}$  can be attributed to the bending vibrational modes (wagging, twisting and rocking) of coordinated water molecules.

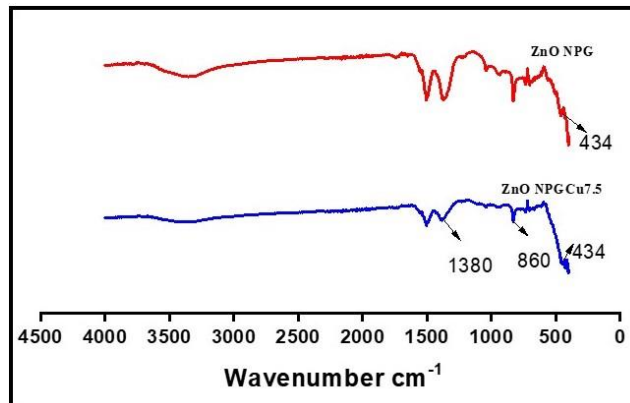


Figure 2. FTIR spectra of ZnONPG & ZnONPGCu(7.5).

#### 3.3. UV-vis Spectroscopy

The UV-vis absorption spectra of the samples are recorded in the wavelength range of 200 to 750 nm. The UV-vis spectra of samples are shown in Figure 3.

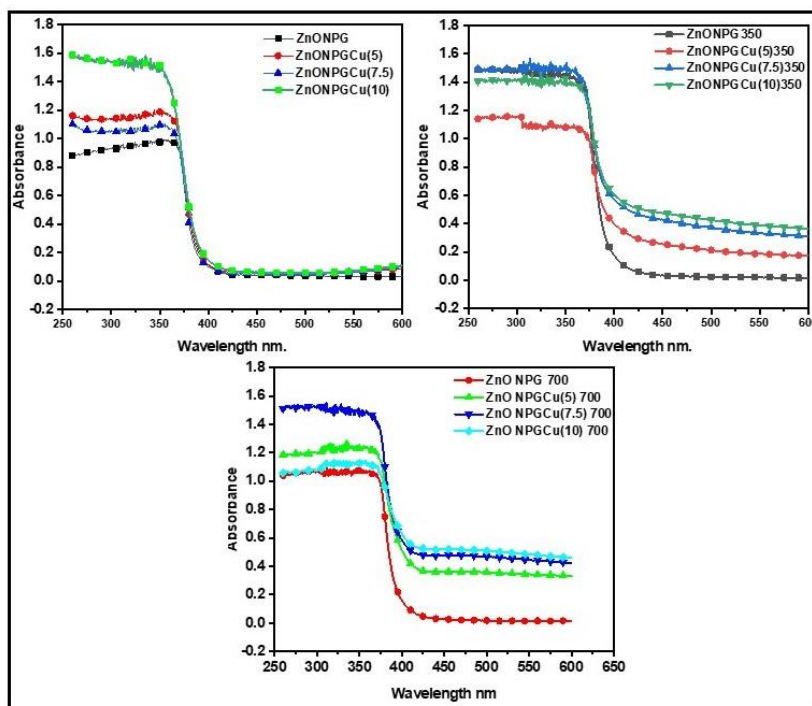


Figure 3. UV-vis spectra of ZnONPG and Cu-doped unannealed and annealed samples.

All the samples have strong absorption below 400 nm. It can be seen that a slight blue shift is observed in Cu-doped

nano zinc oxides. The optical band gap of the nanocrystals can be obtained by analyzing the adsorption edges and by apply-

ing the Tauc model [17] represented by the following relation (1):

$$\alpha h\nu = B(h\nu - E_g)^{1/2} \quad (1)$$

where  $h$  is Planck's constant,  $\nu$  is the frequency of incident photons, and  $B$  is a constant that depends on the electron-hole mobility.

Figure 4 shows the plots of  $(\alpha h\nu)^2$  as a function of the photon energy for the prepared ZnO samples. The band gap energy is obtained by extrapolating the straight line portion of the plot to zero absorption coefficient. In the case of non-annealed samples, the band gap energy values are enhanced on Cu doping. But the band gap energy values of the samples are reduced to a greater extent on annealing as can be seen from the figures.

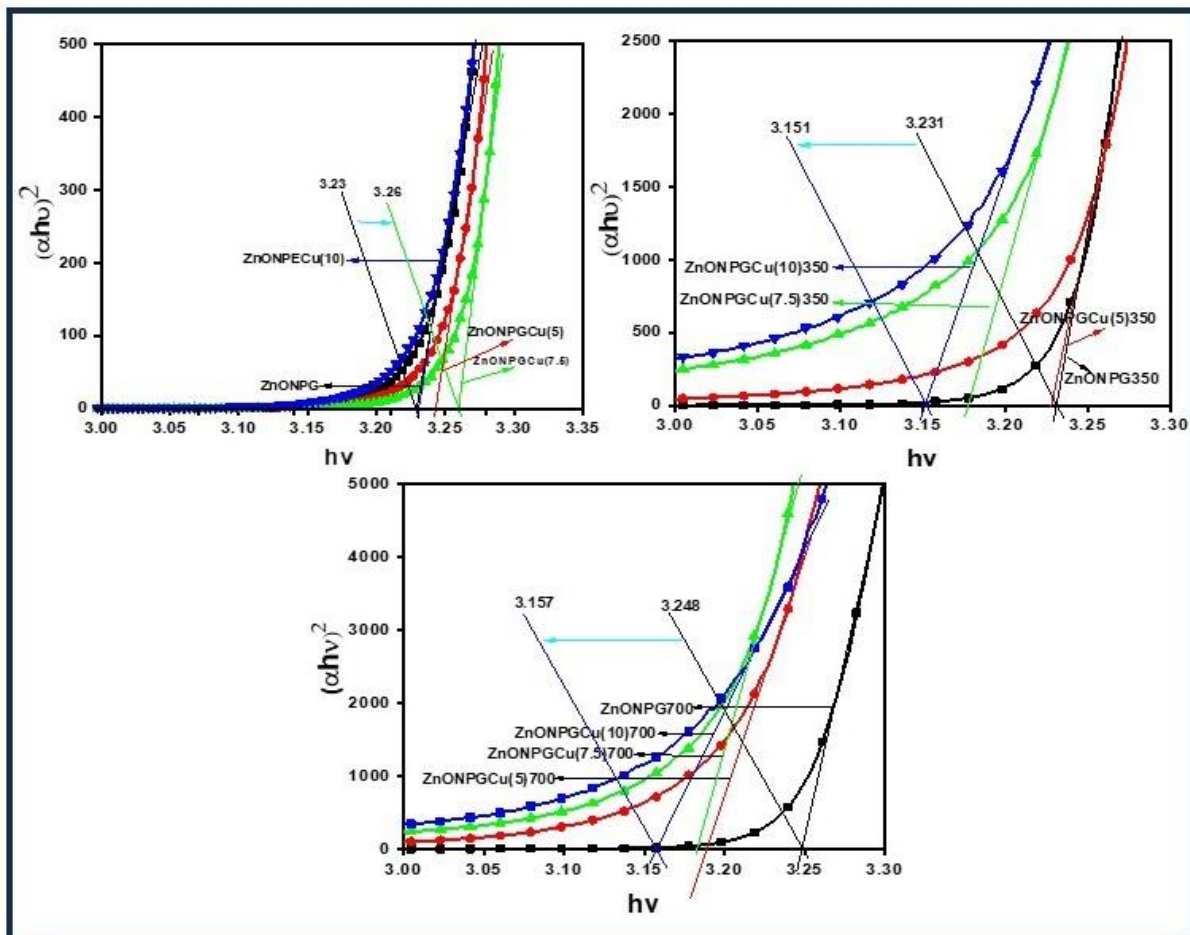


Figure 4. Tauc plot for band gap determination of ZnONPG and ZnONPGCus.

The band gap energy values of the samples from the extrapolation of the straight line portion are shown in Table 1.

Table 1. Band gap energy of synthesized samples.

Samples	Band gap of unannealed samples (eV)	Band gap of samples annealed at 350 °C (eV)	Band gap of samples annealed at 700 °C (eV)
ZnONPG	3.230	3.231	3.248
ZnONPGCu(5)	3.241	3.228	3.189
ZnONPGCu(7.5)	3.258	3.175	3.182
ZnONPGCu(10)	3.231	3.151	3.157

The band gap energies are in good agreement with the reported values [18]. The unannealed Cu-doped ZnO samples show a slight increase in the band gap energy values compared to the neat sample. But on annealing, it can be seen that band gap energies for the Cu-doped samples are decreased appreciably compared to ZnONPG. The annealing influence on band gap energy is not seen in the ZnONPG. The Cu-doped ZnO samples exhibit prominent decrease in the band gap energy. The magnitude of the decrease in band gap energy increases with the increase in concentration of Cu. However, the samples annealed at 350 °C and 700 °C do not show any marginal difference. The decrease in the band gap energy may be due to the increase in the grain size. When the grain size increases, the band gap energy is found to be decreased, which is due to the quantum confinement [19]. At high temperatures, the grain size of the nanoparticles is increased as is evident from the XRD studies.

### 3.4. XRD Analysis

Figure 5 represents the XRD patterns of ZnONPG, Cu-doped nano zinc oxides, synthesized by varying concentrations of Zn<sup>2+</sup> ions and Cu<sup>2+</sup> ions in the presence of plant extract, and samples annealed at 700 °C. The diffraction peaks at scattering angles ~ 31.80°; 34.40°; 36.30°; 47.50°; 56.50°; 62.70° and 67.90° correspond to the reflections from (100), (002), (101), (102), (110), (103) and (112) crystal planes respectively. Well-crystallized diffraction peaks are observed from the XRD pattern. The XRD pattern of all annealed samples is almost similar. It can be seen that the annealed samples contain an additional peak at 38.67°. Nano CuO particles show a strong peak at ~38.60°. This indicates a heterophase formation on annealing. The absence of this peak in unannealed samples may be due to the complexation of some of the Cu<sup>2+</sup> with phytochemicals present in the plant extract. But on annealing these complexes might have decomposed to CuO.

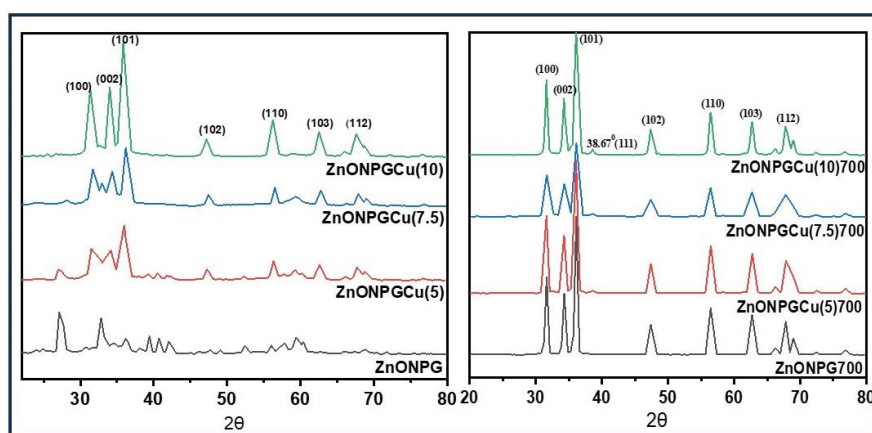


Figure 5. XRD patterns of ZnONPG and Cu-doped ZnONPGs.

The average crystallite size is calculated from the Debye Scherrer formula and Table 2 shows the average crystallite size of ZnONPG and all Cu-doped nano zinc oxide samples prepared and annealed at 700 °C. The average crystallite size is calculated from the intense peaks of XRD data.

Table 2. Crystallite size of unannealed and annealed samples.

Sample	Particle size (nm) unannealed	Particle size (nm) annealed at 700 °C
ZnONPG	17.77	23.48
ZnONPGCu(5)	17.53	22.23
ZnONPGCu(7.5)	18.75	19.26
ZnONPGCu(10)	17.95	21.02

From Table 2, it can be seen that the particle size is not appreciably changed when copper is doped in ZnO. However, the samples annealed at 700 °C show an increase in grain size. On comparing the particle size of each sample at both conditions, the % increase in particle size is greater for the neat sample compared to Cu-doped samples. The optical band gap of the ZnO samples was blue-shifted with temperatures showing particle size growth.

The lattice constants 'a' and 'c' of the wurtzite structure of ZnO can be calculated using the relations (2) and (3) given below

$$a = \lambda / \sqrt{3} \sin \theta_{100} \quad (2)$$

$$c = \lambda / \sin \theta_{002} \quad (3)$$

where  $\lambda = 1.5402 \text{ \AA}$  is the wavelength of X-ray radiation used,  $d_{hkl}$  is the crystalline surface distance for hkl indices,  $\theta_{100}$  and

$\theta_{002}$  are the angles of diffraction peaks (100) and (002) respectively. The unit cell volume for hexagonal structure can be calculated by the relation (4).

$$v = a^2 c \sin 60^\circ = \sqrt{3} a^2 c / 2 \quad (4)$$

**Table 3.** Lattice parameters of various Cu-doped nano zinc oxide samples prepared.

Sample	a (Å)	c (Å)	Unit volume, v (Å <sup>3</sup> )
ZnONPG	3.266	5.211	48.136
ZnONPGCu(5)	3.279	5.242	48.809
ZnONPGCu(7.5)	3.257	5.223	47.981
ZnONPGCu(10)	3.293	5.264	49.433

The calculated lattice parameters are given in Tables 3 and 4. The evaluated lattice parameters of the samples, from XRD data, are in good agreement with those reported in JCPDS

### 3.5. SEM Characterization

Figure 6 depicts the SEM images of unannealed samples and samples annealed at 700 °C.

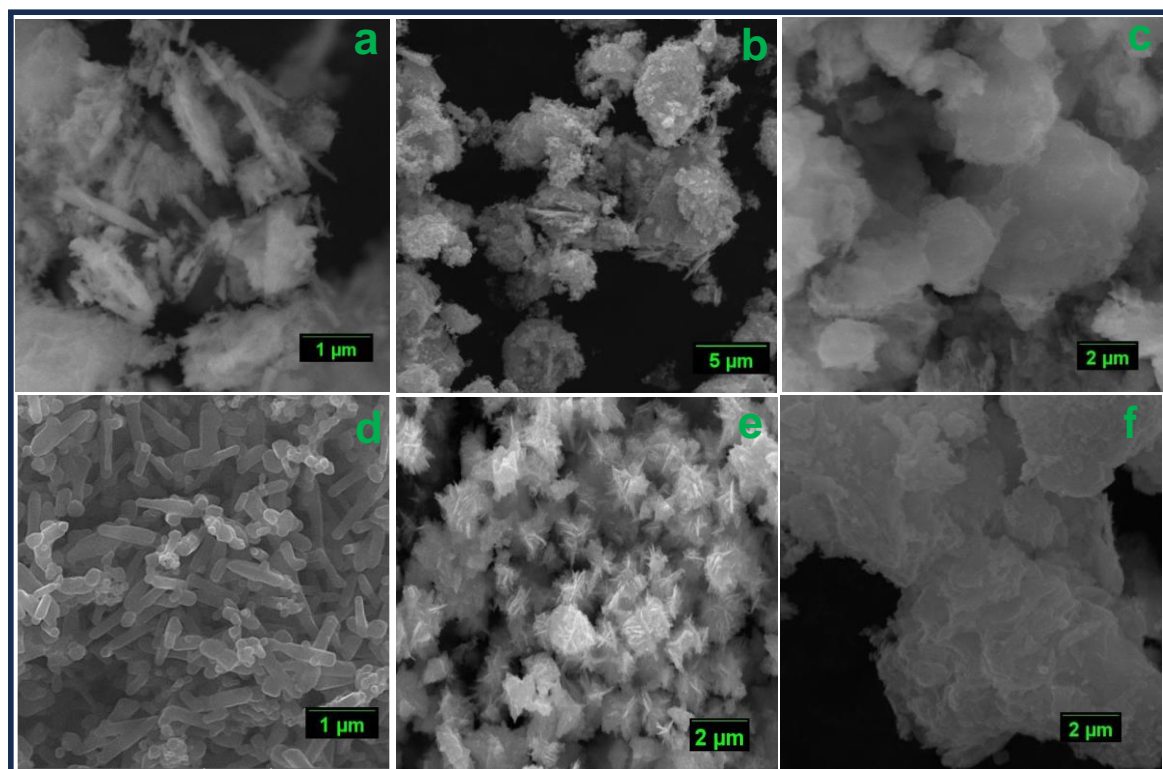


**Figure 6.** SEM images of unannealed and annealed ZnO samples: (a) ZnONPG (b) ZnONPGCu(5) (c) ZnONPGCu(10) (d) ZnONPG700 (e) ZnONPGCu(5)700 (f) ZnONPGCu(10)700.

36-1451 ( $a' = 3.249 \text{ \AA}$ ,  $c' = 5.206 \text{ \AA}$  and  $v' = 47.62 \text{ (\AA)}^3$ ). The slight increase in lattice parameters on doping of  $\text{Cu}^{2+}$  may be due to the non-uniform substitution of  $\text{Cu}^{2+}$  ions into  $\text{Zn}^{2+}$  lattice site even though the ionic radius of  $\text{Cu}^{2+}$  and  $\text{Zn}^{2+}$  ions are almost similar i.e. 7.3 nm & 7.4 nm respectively. Both the doping of Cu to ZnO and the annealing process have not produced any change in the lattice parameters of the ZnO. This indicates the same wurtzite structure is retained under these conditions.

**Table 4.** Lattice parameters of Cu-doped nano zinc oxide samples annealed at 700 °C.

Sample	a (Å)	c (Å)	Unit volume, v (Å <sup>3</sup> )
ZnONPG700	3.264	5.222	48.179
ZnONPGCu(5)700	3.268	5.226	48.334
ZnONPGCu(7.5)700	3.265	5.223	48.217
ZnONPGCu(10)700	3.269	5.227	48.373

The unannealed green synthesized zinc oxide, ZnONPG, contains randomly oriented clustered rod-like structure nanoparticles. The annealing leads to the separation of clustered nanoparticles and the rod-like structure becomes more visible. The morphological features of Cu-doped ZnONPG samples are entirely different from that of neat ZnONPG. The SEM picture of ZnONPGCu(5) shows the presence of nanosheets and these are oriented randomly. This is very clear in the annealed sample and has a flower-like ZnO architecture. Flower has a diameter of  $\sim 2 \mu\text{m}$  and consists of a large number of nanosheets, which are spokewise, projected from a common central zone. The surface morphology ZnONPGCu(10) indicates that the surface is very rough and has nanosheets. This indicates that Cu-doped nano ZnO may be used as a photocatalyst due to greater surface area. The flower-like morphology and sheet-like morphology are clearer in the annealed nano ZnO samples doped with Cu. Thus, it is understood that Cu dopant influences the morphological features of the zinc oxide nanoparticles.

## 4. Conclusion

ZnONP was synthesized by green method in the presence of *Cissus quadrangularis* plant extract. Cu-doped nano zinc oxides were also synthesized in the plant extract medium by varying the concentration of  $\text{Zn}^{2+}$  and  $\text{Cu}^{2+}$  solutions. FTIR confirms the formation of ZnO particles from its characteristic absorption peak of Zn-O stretching at  $\sim 434 \text{ cm}^{-1}$ . ZnONPG and all Cu-doped samples show strong absorption in the UV range, at  $\sim 400 \text{ nm}$ . The optical band gap increases on Cu doping in unannealed samples. On annealing the band gap value decreases with increase in the amount of Cu doping. The green synthesized ZnO samples are crystalline and the particles are in nano regime as indicated by XRD studies. The particle size of ZnONPG and Cu-doped samples is increased on annealing. A slight increase in unit volume reveals the doping of  $\text{Cu}^{2+}$  ions to the  $\text{Zn}^{2+}$  lattice site. The SEM images show that the temperature and Cu-doping alter the morphology of the ZnO nanoparticles.

## Abbreviations

ZnO	Zinc Oxide
ZnONP	Zinc Oxide Nanoparticle
ZnONPG	Zinc Oxide Nanoparticle Green
ZnONPGCu	Zinc Oxide Nanoparticle Green Copper Doped
XRD	X-ray Diffraction
FTIR	Fourier-Transform Infrared Spectroscopy
UV-vis Spectroscopy	Ultraviolet-visible Spectroscopy
SEM	Scanning Electron Microscopy
DMSO	Dimethyl Sulphoxide
CuO	Cupric Oxide

## Acknowledgments

The authors acknowledge the DST, Government of India for the instrumentation facilities provided under the FIST scheme (SR/FIST/College-238/2014(c)).

## Author Contributions

**Parameswaran Parlikad Subramanian:** Conceptualization, Investigation, Methodology, Resources, Writing – review & editing

**Rethikala Pandikkappallil Kumaran:** Data curation, Formal Analysis, Methodology, Validation, Writing – original draft

**Manoj Nageri.:** Formal Analysis, Methodology, Software, Writing – original draft

## Conflicts of Interest

The authors declare no conflicts of interest.

## References

- [1] Z. L. Wang, Nanostructures of zinc oxide, *Materials Today*, 7, 6, 26-33, 2004. [https://doi.org/10.1016/S1369-7021\(04\)00286-X](https://doi.org/10.1016/S1369-7021(04)00286-X)
- [2] Manal Hessien, Recent progress in zinc oxide nanomaterials and nanocomposites: From synthesis to applications, *Ceramics International* 48, 16, 22609-22628, 2022. <https://doi.org/10.1016/j.ceramint.2022.05.082>
- [3] Manoj Gadewar et al, Unlocking nature's potential: Green synthesis of ZnO nanoparticles and their multifaceted applications – A concise overview, *Journal of Saudi Chemical Society*, 28,1, 2024, <https://doi.org/10.1016/j.jscs.2023.101774>
- [4] Sauvik Raha and Md. Ahmaruzzaman, “ZnO nanostructured materials and their potential applications: progress, challenges and perspectives”, *Nanoscale Adv.*, 4, 1868-1925, 2022. <https://doi.org/10.1039/D1NA00880C>
- [5] Morkoc H& Ozgur U, *Zinc Oxide-Fundamental Materials and Device Technology*, 2009 (Wiley-VCH, Weinheim). <https://doi.org/10.1002/9783527623945>
- [6] V. S. Santhosh, K. Rajendra Babu, M. Deepa, Influence of Fe dopant concentration and annealing temperature on the structural and optical properties of ZnO thin films deposited by sol-gel method, *Journal of Material Science: Materials in Electronic*, 25, 224-232, 2014. <https://doi.org/10.1007/s10854-013-1576-5>
- [7] S. Al-Ariki, Nabil A. A. Yahya, Sua'ad A. Al-A'nsi, M. H. Hj Jumali, A. N. Jannah, R. Abd-Shukor, Synthesis and comparative study on the structural and optical properties of ZnO doped with Ni and Ag nanopowders fabricated by sol gel technique, *Scientific Reports*, 11, 11948, 2021. <https://doi.org/10.1038/s41598-021-91439-1>

- [8] Karimi, M., Ezzati, M., Akbari, S. and Behtaj Lejbini, M. ZnO Microparticles, ZnO Nanoparticles and Zn<sub>0.9</sub>Cu<sub>0.1</sub>O Nanoparticles toward Ethanol Vapour Sensing: A Comparative Study. *Current Applied Physics*, 13, 1758-1764, 2013. <https://doi.org/10.1016/j.cap.2013.07.014>
- [9] Xu, C. X., Sun, X. W., Zhang, X. H., Ke, L. & Chua, S. J. Photoluminescent properties of copper-doped zinc oxide nanowires. *Nanotechnology*, 15, 856-861, 2004. <https://doi.org/10.1088/0957-4484/15/7/026>
- [10] M. S. Takumoto, S. H. Pulcinelli, C. V. Santilli, V. Briois, Catalysis and temperature dependence on the formation of ZnO nanoparticles and of zinc acetate derivatives prepared by sol-gel route, *Journal of Physical Chemistry B*, 107, 568, 2003. <https://doi.org/10.1021/JP0217381>
- [11] C. Dhand, N. Dwivedi, X. J. Loh, A. N. J. Ying, N. K. Verma, R. W. Beuerman, R. Lakshminarayanan, S. Ramakrishna, Methods and strategies for the synthesis of diverse nanoparticles and their applications: A comprehensive overview, *Rsc Adv.*, 5, 105003-105037, 2015. <https://doi.org/10.1039/c5ra19388e>
- [12] Barzinjy, A. A., Azeez, H. H. Green synthesis and characterization of zinc oxide nanoparticles using Eucalyptus globulus Labill. leaf extract and zinc nitrate hexahydrate salt. *SN Appl. Sci.* 2., 991, 2020. <https://doi.org/10.1007/s42452-020-2813-1>
- [13] Bouttier-Figueroa, D. C., Cortez-Valadez, M., Flores-Acosta, M. et al. Green Synthesis of Zinc Oxide Nanoparticles Using Plant Extracts and Their Antimicrobial Activity, *Bio Nano Sci.*, 2024. <https://doi.org/10.1007/s12668-024-01471-4>
- [14] Mohd Yusof, H., Mohamad, R., Zaidan, U. H. et al. Microbial synthesis of zinc oxide nanoparticles and their potential application as an antimicrobial agent and a feed supplement in animal industry: a review, *J Animal Sci Biotechnol* 10, 57, 2019. <https://doi.org/10.1186/s40104-019-0368-z>
- [15] Ashwini Jayachandran, Aswathy T. R., Achuthsankar S. Nair, Green synthesis and characterization of zinc oxide nanoparticles using Cayratia pedata leaf extract, *Biochemistry and Biophysics Reports*, 26, 100995, 2021. <https://doi.org/10.1016/j.bbrep.2021.100995>
- [16] Jeganath Sundaran, Raleena begum, Muthu Vasanthi, Manjalam Kamalopathy, Giridharan Bupesh, and Uttamkumar Sahoo, A short review on pharmacological activity of *Cissus quadrangularis*, *Bioinformation*, 16, 8, 579-585, 2020. <https://doi.org/10.6026/97320630016579>
- [17] Khagendra P. Bhandari, Dhurba R. Sapkota, Manoj K. Jamarkattel, Quenton Stillion, Robert W. Collins, Zinc Oxide Nanoparticles—Solution-Based Synthesis and Characterizations, *Nanomaterials*, 13, 11, 1795, 2023. <https://doi.org/10.3390/nano13111795>
- [18] B. Ismail, M. Abaab, B. Rezig, Structural and electrical properties of ZnO films prepared by screen printing technique, *Thin solid films*, 92, 383, 2001. [https://doi.org/10.1016/S0040-6090\(00\)01787-9](https://doi.org/10.1016/S0040-6090(00)01787-9)
- [19] Abduelwhab. B. Alwany, G. M. Youssef, O. M. Samir, Mohammed A. Algrade, Nabil A. A. Yahya, Mohamed A. Swillam, Syahrul Humaidi, R. Abd-Shukor, Annealing temperature effects on the size and band gap of ZnS quantum dots fabricated by co-precipitation technique without capping agent, *Scientific Reports*, 13, 10314, 2023. <https://doi.org/10.1038/s41598-023-37563>